Eur. Phys. J. B **27**, 435–442 (2002)
DOI: 10.1140/epjb/e2002-00175-0

THE EUROPEAN PHYSICAL JOURNAL B

Growth instabilities of vapor deposited films: atomic size versus deflection effect

M. Raible[a], S.J. Linz, and P. Hänggi

Theoretische Physik I, Institut für Physik, Universität Augsburg, 86135 Augsburg, Germany

Received 12 December 2001
Published online 6 June 2002 –

Abstract. Two previously suggested, physically distinct mechanisms for a growth instability of vapor deposited films, the finite atomic size effect and the particle deflection effect due to interatomic attraction, are reconsidered, further analyzed, and compared. We substantiate why the instability caused by interatomic attraction must be considered as the truly underlying instability mechanism. We demonstrate that aspects of the structure zone model of Movchan and Demchishin can also be consistently explained using the growth instability induced by particle deflection instead of the instability arising from the atomic size effect. Most significantly we show that, for vapor deposited amorphous $Zr_{65}Al_{7.5}Cu_{27.5}$-films, the growth instability due to the atomic size effect cannot be present.

PACS. 68.55.-a Thin film structure and morphology – 81.15.Aa Theory and models of film growth

1 Introduction

The preparation and properties of thin films constitute an important field of scientific research and its technological applications. Since the condensation of the films happens far from equilibrium, the structure and the properties of the films depend strongly on the deposition process. Therefore, the understanding of the mechanisms leading to the formation of films has attracted considerable interest [1–5]. Experimental investigations have resulted in a classification of the film structure as it depends on the deposition parameters, especially the substrate temperature [3–5]. Such a classification can help to identify the relevant mechanisms during the growth process of the films. For instance, activation energy determinations have revealed the importance of bulk diffusion at higher substrate temperature [4], whereas at intermediate temperature surface diffusion is the dominant process [3]. In the latter case, roughening due to the deposition of particles then competes with smoothing due to surface diffusion. The surface can evolve into self-similar structures or, in the presence of a growth instability, into a pattern with some intrinsic periodicity. Leamy *et al.* [6] suggested that the finite size of the atoms induces a growth instability of the type $\sim -\nabla^2 H$ (where $H(\boldsymbol{x}, t)$ denotes the coarse-grained surface morphology) because arriving atoms are attached to the surface at a position separated from their center of mass. Mazor *et al.* [7–9] took up this idea in order to predict the surface morphology of vapor deposited films of zone II microstructure and to estimate the zone I to zone II transition temperature in the zone model of Movchan and Demchishin [3]. They argued that this growth instability overcomes the effect of the surface diffusion below the transition temperature, leading to the porous structures of zone I.

On the other hand, Shevchik [10] suggested that a different instability caused by particle deflection due to interatomic attraction gives rise to the growth of surface irregularities on vapor deposited amorphous films. This can lead to the formation of voids when surface diffusion is suppressed.

The aim of this paper is twofold. First, in Section 2, by carefully reconsidering the afore-mentioned mechanisms, we substantiate on theoretical grounds (i) why the atomic size effect is not a feasible option to trigger a growth instability and (ii) that the deflection effect must be considered as the genuine mechanism for that instability. Second, in Section 3, even putting aside the arguments in Section 2 for the moment, we demonstrate that (i) recent experimental data on vapor deposited amorphous $Zr_{65}Al_{7.5}Cu_{27.5}$ films cannot be consistently explained by the atomic size effect and (ii) the transition temperature T_1 between zone I and zone II microstructures of the structure zone model of Movchan and Demchishin previously interpreted by the instability arising from the atomic size effect can also be consistently explained by the deflection effect. Section 4 summarizes the results of our study.

2 Different growth instabilities

2.1 Finite atomic size effect

Mazor *et al.* [7–9] and, earlier, Leamy *et al.* [6] suggested that the finite extension of the deposited atoms (of radius δ) can lead to an unstable growth of the surfaces of

[a] e-mail: martin.raible@physik.uni-augsburg.de

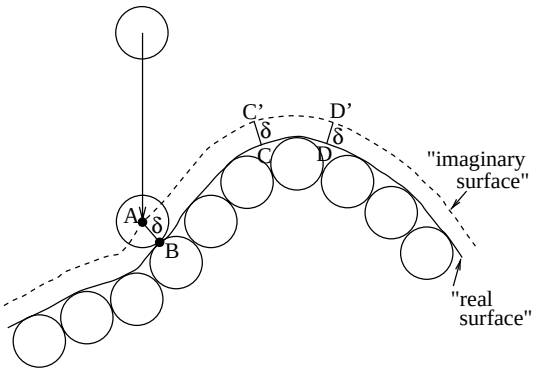

Fig. 1. Sketch of the growth instability attributed to the finite size of the atoms [6–9]: If a particle is deposited on the "real surface" it is actually (with its center of mass) deposited on the "imaginary surface" that is separated by the atomic radius δ from the "real surface". As a consequence, it seems that the segment $C - D$ of the "real surface" receives an increased particle flux due to its negative curvature $\nabla^2 H < 0$.

vapor deposited films. They argued that, if a particle is deposited on the surface $H(\boldsymbol{x}, t)$, this deposition actually takes place on an imaginary surface that is displaced by $\delta \boldsymbol{n}(\boldsymbol{x}, t)$ from the real surface $(\boldsymbol{x}, H(\boldsymbol{x}, t))$; see Figure 1. Here, $\boldsymbol{n}(\boldsymbol{x}, t)$ denotes the unit vector perpendicular to the surface and reads

$$\boldsymbol{n} = \frac{1}{\sqrt{1 + (\nabla H)^2}} \begin{pmatrix} -\nabla H \\ 1 \end{pmatrix}. \tag{1}$$

From this purely geometric consideration, the authors of references [6–9] concluded that, depending on the surface curvature, the flux of particles onto a part of the real surface is either increased or decreased, as shown in Figure 1.

One possible way to derive a quantitative expression for the suggested local change of the deposition rate goes as follows: The imaginary surface can be parametrized by

$$\boldsymbol{x}' = \boldsymbol{x} - \frac{\delta}{\sqrt{1 + (\nabla H)^2}} \nabla H, \tag{2}$$

$$H' = H + \frac{\delta}{\sqrt{1 + (\nabla H)^2}}. \tag{3}$$

Then, the deposition rate on a part of the real surface is changed by the functional determinant of the right-hand side of equation (2) given by

$$\alpha = \det \begin{pmatrix} 1 - \delta \partial_x \frac{\partial_x H}{\sqrt{1+(\nabla H)^2}} & -\delta \partial_y \frac{\partial_x H}{\sqrt{1+(\nabla H)^2}} \\ -\delta \partial_x \frac{\partial_y H}{\sqrt{1+(\nabla H)^2}} & 1 - \delta \partial_y \frac{\partial_y H}{\sqrt{1+(\nabla H)^2}} \end{pmatrix}. \tag{4}$$

Since the atomic radius δ is usually very small compared to the radii of the surface curvature, the correction proportional to δ^2 can be neglected, yielding

$$\alpha = 1 - \delta \nabla \cdot \left(\frac{\nabla H}{\sqrt{1 + (\nabla H)^2}} \right). \tag{5}$$

Therefore, the initially uniform deposition rate F is changed to

$$F\alpha = F - F\delta \nabla \cdot \left(\frac{\nabla H}{\sqrt{1 + (\nabla H)^2}} \right). \tag{6}$$

In addition, the curvature dependent surface diffusion as suggested by Mullins [11] must also be taken into account. Therefore, the complete growth equation for the surface evolution of vapor deposited films that has been proposed by Mazor *et al.* [7,8] reads in one spatial dimension

$$\partial_t H = F - F\delta \partial_x \left(\frac{\partial_x H}{\sqrt{1 + (\partial_x H)^2}} \right) - D_e \partial_x \left[\frac{1}{\sqrt{1 + (\partial_x H)^2}} \partial_x^2 \left(\frac{\partial_x H}{\sqrt{1 + (\partial_x H)^2}} \right) \right]. \tag{7}$$

Here, $D_e = D_s \gamma \Omega^2 \nu / k_B T$ denotes the effective surface diffusion constant where D_s is the coefficient of surface diffusion, γ is the surface-free energy per unit area, Ω is the atomic volume, ν is the number of atoms per unit area, and T is the surface temperature [11].

If the initial height distribution $H(x, 0)$ is almost flat, useful insights into the early stages of the surface evolution predicted by equation (7) can be obtained from its linearized version

$$\partial_t H = F - F\delta \partial_x^2 H - D_e \partial_x^4 H. \tag{8}$$

A perturbation of the form $\sin(kx)$ grows or decays exponentially with the growth rate $\sigma(k) = F\delta k^2 - D_e k^4$. Therefore, all perturbations with wavelengths $\lambda > \lambda_0 = 2\pi\sqrt{D_e/F\delta}$ increase until the nonlinear terms of equation (7) begin to influence the evolution of the height profile [7,8].

2.2 Deflection of particles due to interatomic forces

Next, we discuss an alternative scenario leading to a growth instability that has been suggested by Shevchik [10] for the spatio-temporal evolution of amorphous films. Here, the key idea is that the particles initially move in a direction being perpendicular to the substrate towards the film, but, when they are close to the surface, they are attracted by interatomic forces towards the surface. As a consequence, more particles arrive at places with negative curvature $\nabla^2 H < 0$ than at places with positive curvature $\nabla^2 H > 0$, as shown in Figure 2. The attractive forces between the oncoming particles and the already condensed atoms at the surface are the same forces that hold the solid together [10]. For experimental indications of the relevance of this effect we refer to [12,13], for its relevance in the context of crystal growth *cf.* the recent simulations in reference [14].

In order to derive a quantitative expression for the effect of the particle deflection on the evolution of the height profile $H(\boldsymbol{x}, t)$, we use the idealization that this deflection

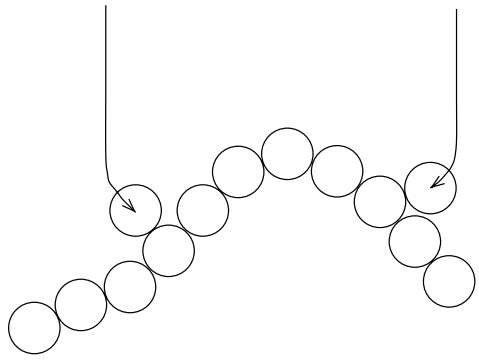

Fig. 2. Sketch of the deflection effect [10]: When the particles are close to the surface they are attracted by interatomic forces in a direction perpendicular to the surface. Consequently, more particles arrive on mounds than on valleys.

(in a direction perpendicular to the surface) happens instantaneously when a particle arrives at a distance b from the surface [15], as shown in Figure 3. This idealization is reasonable if the initial kinetic energy of the particles (typically a few tenths of an eV in physical vapor deposition experiments) is small compared to their binding energy on the surface (typically a few eVs). Here, the parameter b characterizes the effective range of the interatomic forces and depends on the specific details of the interaction potential and the initial kinetic energy of the particles (*cf.* the Appendix for a quantitative estimate of b). As shown in Figure 3, b can be larger or smaller than the atomic radius. Using the same mathematical technique as in the previous section and again adding the contribution of the surface diffusion, we obtain the surface evolution equation

$$\partial_t H = F - Fb\partial_x \left(\frac{\partial_x H}{\sqrt{1+(\partial_x H)^2}} \right) - D_e \partial_x \left[\frac{1}{\sqrt{1+(\partial_x H)^2}} \partial_x^2 \left(\frac{\partial_x H}{\sqrt{1+(\partial_x H)^2}} \right) \right] \tag{9}$$

for vapor deposited films in the presence of particle deflection and surface diffusion in the one-dimensional case, or, after linearization,

$$\partial_t H = F - Fb\partial_x^2 H - D_e \partial_x^4 H. \tag{10}$$

2.3 Comparison of the growth instabilities

The two presented growth instabilities are based on rather distinct physical arguments: The atomic size effect constitutes a purely geometric argument (no interaction involved) and the entering parameter δ is fixed by the size of the deposited atoms. In contrast to that, the deflection effect results from the ubiquitous atomic interaction. The similarity of the mathematical description of the two effects, *cf.* equations (8, 10), is only the result of the simplified model that we have used in order to quantitatively

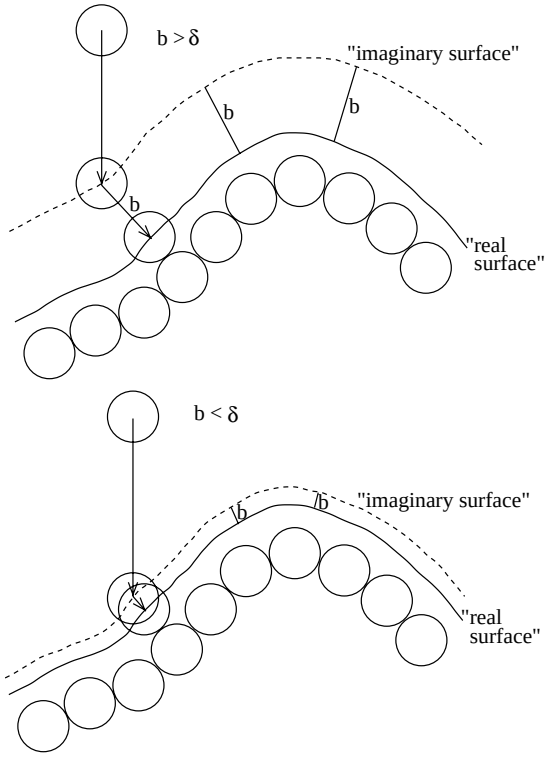

Fig. 3. Idealization of the deflection effect: In a simplified model, the particle changes instantaneously its direction when it arrives at a distance b from the surface where b characterizes the typical range of the interatomic forces. In the upper (lower) part of the figure, b is larger (smaller) than the atomic radius δ.

estimate the effect of the particle deflection. Another striking difference is that the "imaginary surface" of Figure 1 coincides with the "real surface" that is defined in Figure 3. We find the definition of the "real surface" given in Figure 3 more satisfactory because the oncoming particles are effectively deposited on this surface and diffuse along it.

Next, we reexamine the growth instability due to the finite size effect of the deposited atoms. The absence of particle desorption implies a balance of the mass equation

$$\partial_t c = \rho_0[-\nabla \cdot \boldsymbol{j} + F] \tag{11}$$

where $c(\boldsymbol{x}, t)$ denotes the number of atoms of the film per substrate area above a given substrate position $\boldsymbol{x}$. Allowing for possible density variations that depend on the surface inclination, but not on the surface curvature, the rate of change of c is related to the rate of change of H by $\partial_t c = \rho(\nabla H)\partial_t H$. Here $\rho(\nabla H)$ denotes the density of the film close to the surface. Dividing equation (11) by $\rho(\nabla H)$ leads to

$$\partial_t H = \frac{\rho_0}{\rho(\nabla H)}[-\nabla \cdot \boldsymbol{j} + F]. \tag{12}$$

This equation shows that, if no particle desorption from the surface occurs and curvature dependent density variations in the growing film can be neglected, a growth

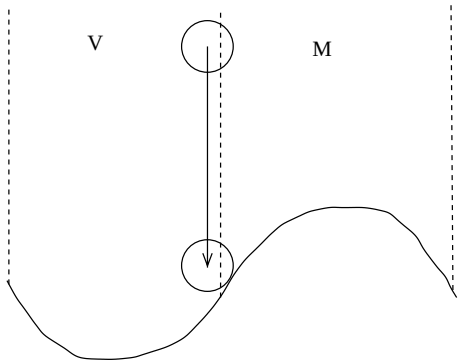

Fig. 4. Without the influence of the interatomic attraction the particle does not traverse the boundary between the area of the valley V and the area of the mound M. It only "looks" into area M. This again shows that the finite atomic size cannot cause a growth instability.

instability of the type $-\nabla^2 H$ must necessarily be the result of a mass current of the form $\boldsymbol{j} \sim \nabla H$. However, the atomic size *does not cause a mass transport* parallel to the substrate, as shown in Figure 1. The current $\boldsymbol{j} \sim \nabla H$ that is included in the model equations (7, 8) is essentially the result of an unjustified change in the description of the particle position. Before deposition, the location of the particle is described by the coordinates of its center of mass, but after deposition, the particle position is described by the place where it sticks to the surface. This leads to a *fictive* motion from point A to point B in Figure 1. In contrast to that, the interatomic attraction results in a *real* motion of the particle in the direction of the height gradient, as shown in the Figures 2 and 3. Since only real displacements of particles count in the growth equation, we conclude that the finite atomic size effect is unable to cause a growth instability.

This statement can be further substantiated by the following, simple consideration. In Figure 4 we show a height profile that possesses a valley in area V and a mound in area M. In the presence of a growth instability particles should traverse the boundary from V to M in order to enhance the height increase of the mound. However, the particle shown in Figure 4 (without the inflection of its trajectory due to interatomic forces) does not cross the boundary between area V and area M. It only "looks" into area M with a part of its volume. That the particle in Figure 4 sticks to the surface at a place that is on the right of its center of mass does *not* imply that it prefers to diffuse to the right.

3 Comparison with experiments

3.1 Transition temperature between microstructural growth regimes

Since the effective range b of the interatomic forces usually has the same order of magnitude as the atomic radius δ, experimental indications of the relevance of the growth instability based on the finite atomic size effect can also be interpreted as the result of the instability that is caused by the particle deflection. For example, the transition temperature between the zone I and zone II microstructures appearing in the growth of thick vapor deposited films has been derived by Mazor *et al.* [7,8] from the smallest unstable wavelength $\lambda_0 = 2\pi\sqrt{D_e/F\delta}$ of equation (7).

By studying thick films of different metals and metal oxides deposited by evaporation at high rates between $F = 20$ nm/s and $F = 300$ nm/s Movchan and Demchishin [3] identified three structure zones separated by the boundary temperatures T_1 and T_2. Each zone has its own characteristic structure and physical properties. The boundary temperatures are $T_1 \approx 0.3T_m$ for metals, $T_1 \approx (0.22 - 0.26)T_m$ for oxides, and $T_2 \approx (0.45 - 0.5)T_m$ for metals and oxides where T_m is the melting point of the film. At low substrate temperature $T < T_1$ (zone I), the film is porous and consists of tapered crystallites with domed tops which are separated by voided boundaries [3,5]. For $T_1 < T < T_2$ (zone II), the microstructure consists of columnar grains separated by distinct, dense, intercrystalline boundaries. There is no porosity, and the columnar grains have smooth, mat surfaces. The increase of the grain width with temperature T yields the same activation energy as for surface diffusion [3]. Beyond T_2 (zone III), the film consists of equiaxed grains with a bright surface. Here, an activation energy equal to that for bulk diffusion can be estimated from the relationship between the crystallite diameters and the temperature T [4].

The porosity of the zone I microstructures is due to ballistic aggregation at weak surface diffusion. On the other hand, at higher temperature the surface diffusion smoothes the surface, so that overhangs and voided regions do not form. In order to obtain the transition temperature T_1, Mazor *et al.* [7,8] equated the smallest unstable wavelength λ_0 with a few atomic radii, *i.e.* they solved the equation $2\pi\sqrt{D_e/F\delta} = \eta\delta$ where η is an arbitrary number between 1 and 10. Using the temperature dependence of the diffusion coefficient, $D_s = D_0 \exp(-5T_m/T - 20/3)$, they obtained a transition temperature of $T_1 \approx 0.23T_m$ [7,8], being in good agreement with the experimental value. Since the diffusion coefficient D_s increases with temperature, even Fourier modes with a wavelength of an atomic diameter are unstable below this temperature and the surface structure becomes rough on all length scales. This roughness can act as a progenitor for the formation of the voided regions of zone I microstructures.

In order to show that the transition temperature from zone I to zone II microstructures can also be interpreted by means of the growth instability induced by particle deflection, we now use the growth model equation (10) instead of equation (8). Here, the smallest unstable wavelength reads $\lambda_0 = 2\pi\sqrt{D_e/Fb}$. The condition $2\pi\sqrt{D_e/Fb} = \eta\delta$ again yields the same transition temperature $T_1 \approx 0.23T_m$ because b has the same order of magnitude as δ [13] and the coefficient of surface diffusion D_s depends exponentially on the temperature T. Therefore, the growth instability caused by the particle deflection can also lead to an

exponential growth of all physically meaningful Fourier modes if the temperature T is smaller than T_1. In addition, the growth rate of the Fourier modes predicted by equation (10), $\sigma(k) = Fbk^2 - D_e k^4$, takes very large values below the transition temperature T_1. Then, the maximum $F^2b^2/4D_e$ of $\sigma(k)$ that occurs at a wavelength of $\sqrt{2}\lambda_0 = 2\pi\sqrt{2D_e/Fb}$ is larger than $Fb\pi^2/\delta^2\eta^2 \sim F/\delta$. This implies that even after the deposition of a few atomic layers the amplitudes of Fourier modes with a wavelength of a few atomic radii increase by several orders of magnitude. Again, as in the case of the growth instability due to the atomic size effect, the fast increasing surface roughness can act as a progenitor for the formation of voided regions in the film [10], as explained in the next section. Therefore, the successful prediction of the transition temperature between the growth of zone I and zone II microstructures by Mazor *et al.* [7,8] can also be obtained if one uses the growth instability due to the deflection of particle trajectories instead of the growth instability being related to the atomic size.

3.2 The influence of the finite atomic size on the growth of films

A major purpose of this paper is to substantiate that the finite size of the atoms cannot give rise to a linear growth instability of the form $-\nabla^2 H$. However, the finite size of the atoms can influence the growth of vapor deposited films. If the surface diffusion is very small, steep surface areas appear due to the growth instability caused by the particle deflection, the stochasticity of the incident particle flux, or the substrate roughness [5]. On these strongly inclined parts of the surface, protruding atoms cast a shadow upon unoccupied places because of their size. This can lead to the formation of overhangs and finally to the appearance of voided regions in the film. However, *this* finite atomic size effect does not imply a growth instability in the sense that more particles are incorporated on surface mounds than above the troughs. If lower parts of the film surface are overgrown due to shadowing effects this leads to an additional volume increase above the valleys, contrary to the effect of a growth instability of the form $-\nabla^2 H$ in a surface evolution equation.

3.3 Growth instability on vapor deposited amorphous films

The growth instability attributed to the particle deflection effect has been recently observed in vapor deposition experiments of amorphous films. Specifically, a continuum equation of the form

$$\partial_t h = a_1\nabla^2 h + a_2\nabla^4 h + a_3\nabla^2(\nabla h)^2 + a_4(\nabla h)^2 + \eta \tag{13}$$

has been compared to experimental results [13]. Here, $h(\boldsymbol{x},t)$ denotes the height profile in a frame comoving with the deposition velocity F, *i.e.* $h(\boldsymbol{x},t) = H(\boldsymbol{x},t) - Ft$. In the experiments [16–19] amorphous $Zr_{65}Al_{7.5}Cu_{27.5}$-films have been prepared at room temperature in ultra high vacuum by electron beam evaporation with a deposition rate of $F = 0.79$nm/s. The surface morphology of the resulting films has been observed using scanning tunneling microscopy (STM) [16–19]. One observation in reference [13] has been that the linearized version of equation (13)

$$\partial_t h = a_1\nabla^2 h + a_2\nabla^4 h + \eta \tag{14}$$

is sufficient to reproduce the experimental data up to a layer thickness of 240 nm and that the crossover to nonlinear behaviour sets in at a larger layer thickness.

The first term on the right-hand side of equation (14) has been attributed to the growth instability that is induced by particle deflection. Therefore, $a_1 = -Fb < 0$ holds. The second term $a_2\nabla^4 h$ with $a_2 < 0$ is related to the known microscopic mechanism of curvature induced surface diffusion [11,20]. The deposition noise η represents the experimentally unavoidable fluctuations of the particle flux around its mean F and is assumed to be Gaussian white, *i.e.*

$$\begin{aligned}\langle\eta(\boldsymbol{x},t)\rangle &= 0,\\ \langle\eta(\boldsymbol{x},t)\eta(\boldsymbol{y},t')\rangle &= 2D\delta(\boldsymbol{x}-\boldsymbol{y})\delta(t-t')\end{aligned} \tag{15}$$

where the brackets denote ensemble averaging. Equations (13, 14) have been solved on an area $[0,L]^2$ subject to periodic boundary conditions and starting from a flat substrate $h(\boldsymbol{x},0) = 0$. Note that the linearized growth equation (14) possesses one length constant $\sqrt{a_2/a_1}$, one time constant $|a_2/a_1^2|$, and one height constant $\sqrt{D/|a_1|}$.

In order to compare with the experiments we calculated the height-height correlation function

$$\begin{aligned}&C(r,t) =\\ &\langle\langle\langle[h(\boldsymbol{x},t)-\langle h(t)\rangle_{\boldsymbol{x}}][h(\boldsymbol{x}+\boldsymbol{r},t)-\langle h(t)\rangle_{\boldsymbol{x}}]\rangle\rangle_{\boldsymbol{x}}\rangle_{|\boldsymbol{r}|=r}\end{aligned} \tag{16}$$

where $\langle h(t)\rangle_{\boldsymbol{x}} = (1/L^2)\int d^2x h(\boldsymbol{x},t)$ denotes the spatial average of the height, and $\langle\langle\langle\ldots\rangle\rangle_{\boldsymbol{x}}\rangle_{|\boldsymbol{r}|=r}$ denotes a combined ensemble, spatial, and radial average. Then, the square of the surface roughness $w(t)$ is given by the relation $w^2(t) = C(0,t)$, and the correlation length $R_c(t)$ is defined by the radius r of the first maximum of $C(r,t)$ occurring at nonzero r. The quantities $w(t)$ and $R_c(t)$ basically represent the typical height and length scale of the mound-like surface structures arising from equations (13, 14).

The linearized equation (14) reads in Fourier space $\partial_t\tilde{h}(\boldsymbol{k},t) = \sigma(k)\tilde{h}(\boldsymbol{k},t) + \tilde{\eta}(\boldsymbol{k},t)$ where $\sigma(k) = -a_1k^2 + a_2k^4$ denotes the growth coefficient of the Fourier modes. The growth rate $\sigma(k)$ possesses a maximum at the critical wave number $k_c = \sqrt{a_1/2a_2}$. Therefore, the correlation length $R_c(t)$ of the surface structure arising from equation (14) first increases and then saturates into

$$R_c(t) = 7.0156/k_c = 7.0156\sqrt{2a_2/a_1} \tag{17}$$

when the critical mode dominates. Since the experimental results also reveal a saturation of R_c for film thicknesses larger than 200nm (*cf.* the diamond symbols in Fig. 5a),

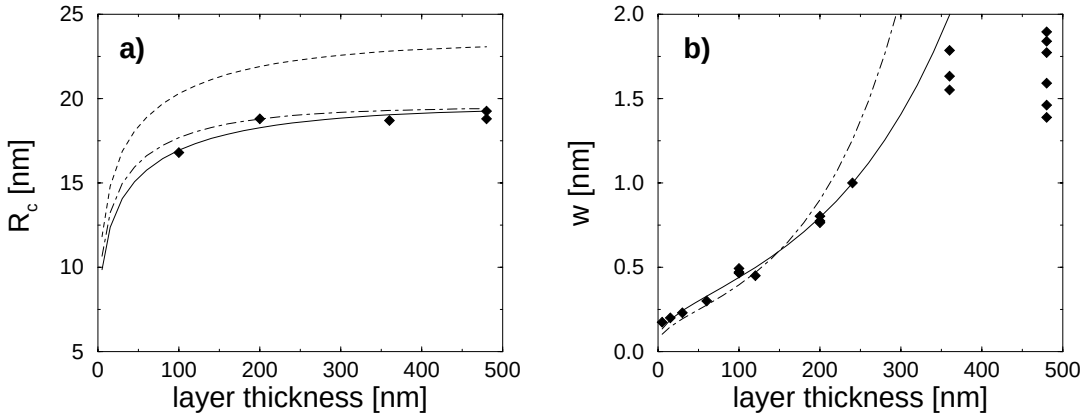

Fig. 5. The solid lines depict the correlation length R_c and surface roughness w calculated from the linearized growth equation (14) using the parameters given in equation (18) as functions of the layer thickness that is determined by Ft. The dashed line shows the correlation length R_c resulting from equation (14) using the parameters $a_1 = -0.119$ nm^2/s, $a_2 = -0.658$ nm^4/s, and $D = 0.0249$ nm^4/s. The dash-dotted lines show the prediction that results from equation (14) using the parameters $a_1 = -0.119$ nm^2/s, $a_2 = -0.459$ nm^4/s, and $D = 0.0119$ nm^4/s. The diamond symbols represent the corresponding experimental results (taken from [16–19]).

the ratio a_2/a_1 can be estimated. The surface roughness $w(t)$ grows exponentially with the growth rate $\sigma(k_c) = -a_1^2/4a_2$, when the critical mode dominates at larger layer thicknesses. Since an exponential growth of $w(t)$ is also observed in the experiments for film thicknesses between 30 nm and 240 nm (*cf.* the diamond symbols in Fig. 5b), the ratio a_1^2/a_2 can also be estimated. From the ratios a_2/a_1 and a_1^2/a_2 the coefficients a_1 and a_2 can roughly be derived. Using a systematic parameter identification procedure that starts from these roughly estimated values of a_1 and a_2 described in reference [13], we have obtained the following parameters

$$a_1 = -0.0826 \text{ nm}^2/\text{s}, \quad a_2 = -0.319 \text{ nm}^4/\text{s}, \\ D = 0.0174 \text{ nm}^4/\text{s}, \tag{18}$$

that fit the experimental results best. The solid lines in Figures 5a and b show the correlation length $R_c(t)$ and the surface roughness $w(t)$ resulting from equation (14) using these parameters. There is obviously a very good agreement with the experimental results up to a layer thickness of $\langle H \rangle \approx 240$ nm. Additionally, using the complete nonlinear growth equation (13), the experimental data at larger film thicknesses $\langle H \rangle \leq 480$ nm could also be reproduced [13]. From the coefficient a_1 given in equation (18) and the relation $a_1 = -Fb$ we have determined the effective range of the interatomic forces given by $b \approx 0.1$ nm. As remarked in reference [13], this value is a little bit smaller than the atomic radii of Zr, Al, and Cu and has therefore a reasonable order of magnitude.

Next, we investigate whether the growth instability arising from the finite atomic size effect can also reproduce the experimental data. In this case, the coefficient a_1 of the equations (13) and (14) is given by the relation $a_1 = -F\delta$ where δ is the atomic radius. The metallic radii, *i.e.* the half of the minimal distance between neighbouring atoms, of the pure elements Zr, Al, and Cu are given by 0.16 nm, 0.143 nm, and 0.128 nm, respectively [21,22]. If we weight these radii according to the stoichiometric composition of the three elements in the $Zr_{65}Al_{7.5}Cu_{27.5}$-films, we obtain an averaged atomic radius of $\delta = 0.15$ nm. This yields a coefficient $a_1 = -0.119$ nm^2/s that exceeds the one given in equation (18) by 44%. If we adjust the other parameters to $a_2 = -0.658$ nm^4/s and $D = 0.0249$ nm^4/s in order to obtain the same time constant $|a_2/a_1^2|$ and the same height constant $\sqrt{D/|a_1|}$ again, the surface roughness $w(t)$ remains unchanged. However, due to an increased length constant $\sqrt{a_2/a_1}$ the correlation length $R_c(t)$ of the height profile arising from equation (14) is then too large compared to the experimental values; see the dashed line in Figure 5a. On the other hand, if we use the coefficient $a_2 = -0.459$ nm^4/s, the length constant $\sqrt{a_2/a_1}$ takes the same value as in equation (18) and $R_c(t)$ is now again in accordance with the experimental data, as shown by the dash-dotted line in Figure 5a. But then the time constant $|a_2/a_1^2|$ is too small and the critical growth rate $\sigma(k_c) = -a_1^2/4a_2$ is too large, leading to a too fast increase of $w(t)$; see the dash-dotted line in Figure 5b. Consequently we conclude that the experimental data on vapor deposited amorphous $Zr_{65}Al_{7.5}Cu_{27.5}$-films (taken from [16–19]) cannot be consistently interpreted if one applies the growth instability attributed to the finite atomic size effect because then the resulting coefficient $a_1 = -F\delta$ in equation (14) would have a far too large absolute value. This outcome corroborates the fact that a growth instability $-F\delta\nabla^2 h$ arising from the finite atomic size effect cannot be present.

4 Conclusions

In this study we have reconsidered two possible mechanisms for a growth instability of vapor deposited films: (i) the effect of the finite size of the atoms [6–9] and (ii) the effect of particle deflection due to interatomic attraction [10]. We have argued on theoretical grounds

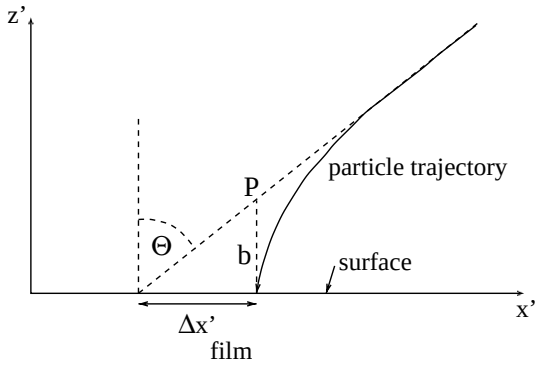

Fig. 6. Sketch of the deflection effect (in the local coordinate system of the surface). The particle hits the surface at a position that is displaced by a distance $\Delta x'$ from the disposal position for $V(z') \equiv 0$. The attractive interaction potential $V(z') < 0$ possesses a minimum at $z' = 0$. Therefore, the x'-axis of this figure lies in the "real surface" that is defined in Figure 3 where the attractive and repulsive forces from the already condensed surface atoms onto the arriving particle compensate each other.

why the instability caused by particle attraction seems to be the physically relevant one. Further, we have illustrated by an example that experimental indications of the growth instability due to the finite atomic size effect can also be consistently attributed to the instability induced by the deflection of particle trajectories. Finally, we have shown for the specific case of vapor deposited amorphous $Zr_{65}Al_{7.5}Cu_{27.5}$-films that the growth instability due to interatomic attraction leads to a consistent explanation of experimental data [16–19], whereas the other growth instability cannot be present. This corroborates our theoretical reasoning that the atomic size effect is not a substantial instability mechanism.

This work has been supported by the DFG-Sonderforschungsbereich 438 München/Augsburg, TP A1. We also thank S.G. Mayr, M. Moske, and K. Samwer for interesting discussions.

Appendix A: Estimation of the effective range of the interatomic forces

Here, we present a derivation of the effective range of the interatomic forces b in terms of the attractive interaction potential and the initial kinetic energy of the particles. Let us suppose that the film surface is flat, but oblique compared to the particle beam, as shown in Figure 6. Consider a particle that travels from a large distance towards the film. Initially, the angle between the particle direction and the direction perpendicular to the surface is Θ. On its way, the particle changes its direction due to the attractive interaction potential $V(z') < 0$. Therefore, the particle hits the surface at a point that is displaced by a distance

$$\Delta x' = \int_0^\infty \mathrm{d}z' \left(\tan(\Theta) - \frac{v_x}{v_z} \right) \tag{19}$$

from the disposal point for $V(z') \equiv 0$. Here, v_x and v_z denote the velocities of the particle in the x'- and z'-direction. The velocity component in the surface direction $v_x = -v_0 \sin(\Theta)$ remains unchanged where v_0 denotes the initial velocity of the particle. In contrast to that, the velocity component perpendicular to the surface v_z depends on the distance z' to the surface because of the conservation of energy:

$$\frac{1}{2} m v_z^2 + V(z') = \frac{1}{2} m v_0^2 \cos^2(\Theta). \tag{20}$$

Therefore, $v_z(z') = -\sqrt{v_0^2 \cos^2(\Theta) - 2V(z')/m}$ holds, yielding

$$v_x / v_z = \sin(\Theta) / \sqrt{\cos^2(\Theta) - V(z')/E_{kin}} \tag{21}$$

where $E_{kin} = m v_0^2/2$ represents the kinetic energy of the particle before the interaction with the surface atoms. This leads to

$$\Delta x' = \int_0^\infty \mathrm{d}z' \left(\tan(\Theta) - \frac{\sin(\Theta)}{\sqrt{\cos^2(\Theta) - V(z')/E_{kin}}} \right) . \tag{22}$$

The effective range of the interaction b can be obtained if one supposes that the particle first moves straight and then, at a distance b from the surface (at point P in Fig. 6), suddenly turns into a direction perpendicular to the surface. Therefore, b is given by

$$b(\Theta) = \frac{\Delta x'}{\tan(\Theta)} = \int_0^\infty \mathrm{d}z' \left(1 - \frac{1}{\sqrt{1 - V(z')/(E_{kin} \cos^2(\Theta))}} \right) . \tag{23}$$

Note that $b(\Theta)$ increases with increasing angle Θ. At $\Theta = 90°$ there is even $b(\Theta) = +\infty$. This, however, is only a consequence of the unrealistic assumption that the inclined surface area is flat and infinite and leads to unrealistic results at large angles of inclination Θ. At small Θ, $b(\Theta)$ is basically independent of Θ:

$$b \approx \int_0^\infty \mathrm{d}z' \left(1 - \frac{1}{\sqrt{1 - V(z')/E_{kin}}} \right) . \tag{24}$$

This equation shows how b depends on the interaction potential $V(z')$ and the initial kinetic energy of the particles E_{kin}. The resulting effective range of the interatomic forces b is approximately determined by the distance from the surface where the absolute value of the attractive interaction potential becomes smaller than the initial kinetic energy.

References

1. A.L. Barabasi, H.E. Stanley, *Fractal Concepts in Surface Growth* (Cambridge University Press, Cambridge, 1995); W.M. Tong, R.S. Williams, Annu. Rev. Phys. Chem. **45**, 401 (1994); J. Krug, Adv. Phys. **46**, 139 (1997); M. Marsili, A. Maritan, F. Toigo, J.R. Banavar, Rev. Mod. Phys. **68**, 963 (1996)
2. J. Villain, J. Phys. I France **1**, 19 (1991)
3. B.A. Movchan, A.V. Demchishin, Phys. Met. Metallogr. **28**, 83 (1969)
4. B.A. Movchan, A.V. Demchishin, L.D. Kooluck, J. Vac. Sci. Technol. **11**, 869 (1974)
5. J.A. Thornton, Ann. Rev. Mater. Sci. **7**, 239 (1977)
6. H.J. Leamy, G.H. Gilmer, A.G. Dirks, in *Current Topics in Materials Science*, Vol. 6, edited by E. Kaldis (North-Holland, Amsterdam, 1980), p. 309
7. A. Mazor, D.J. Srolovitz, P.S. Hagan, B.G. Bukiet, Phys. Rev. Lett. **60**, 424 (1988)
8. D.J. Srolovitz, A. Mazor, B.G. Bukiet, J. Vac. Sci. Technol. A **6**, 2371 (1988)
9. A. Mazor, B.G. Bukiet, D.J. Srolovitz, J. Vac. Sci. Technol. A **7**, 1386 (1989)
10. N.J. Shevchik, J. Non-Cryst. Solids **12**, 141 (1973)
11. W.W. Mullins, J. Appl. Phys. **28**, 333 (1957)
12. S. van Dijken, L.C. Jorritsma, B. Poelsema, Phys. Rev. Lett. **82**, 4038 (1999)
13. M. Raible, S.G. Mayr, S.J. Linz, M. Moske, P. Hänggi, K. Samwer, Europhys. Lett. **50**, 61 (2000)
14. F. Montalenti, A.F. Voter, Phys. Rev. B **64**, 081401 (R) (2001); F. Montalenti, M.R. Sørensen, A.F. Voter, Phys. Rev. Lett. **87**, 126101 (2001)
15. M. Raible, S.J. Linz, P. Hänggi, Phys. Rev. E **62**, 1691 (2000)
16. S.G. Mayr, M. Moske, K. Samwer, Mater. Sci. Forum **343-346**, 221 (2000)
17. S.G. Mayr, M. Moske, K. Samwer, *The growth of vapor deposited amorphous ZrAlCu-alloy films: Experiment and simulation*, Lectures on Applied Mathematics, edited by H.-J. Bungartz, R.H.W. Hoppe, C. Zenger (Springer, Berlin, Heidelberg, 2000), p. 233
18. B. Reinker, M. Moske, K. Samwer, Phys. Rev. B **56**, 9887 (1997)
19. B. Reinker, *STM-Untersuchungen an amorphen ZrCo- und ZrAlCu-Aufdampfschichten* (Dissertation, Universität Augsburg, Wißner Verlag, Augsburg, 1996)
20. D.E. Wolf, J. Villain, Europhys. Lett. **13**, 389 (1990)
21. C. Kittel, *Einführung in die Festkörperphysik* (R. Oldenbourg Verlag, München, Wien, 1991)
22. W.B. Pearson, *Lattice Spacings and Structures of Metals and Alloys*, Vol. 2 (Pergamon Press, Oxford, 1967)